The Dynamics of Intramolecular Energy Hopping in Multi-Bodipy Self – Assembled Metallocyclic Species: A Tool For Probing Subtle Structural Distortions in Solution.

Elisabeth Martinou,[1] Kostas Seintis,[2] Nikolaos Karakostas,[1] Anna Bletsou,[3] Nikolaos S. Thomaidis,[3] Mihalis Fakis[2] and George Pistolis*,[1]

[1] *NCSR "Demokritos" Institute of Nanosciences and Nanotechnology (INN) 153 10 Athens, Greece*

[2] *Department of Physics, University of Patras, 26500 Patras, Greece*

[3]*Department of Chemistry, National and Kapodistrian University of Athens, 15771 Athens, Greece*

Table of Contents **page**

Materials and Methods: All chemicals were used without further purification and purchased from commercial sources. The builing blocks M1[1], M2[2] and the rhomboid (A1)[1] were prepared according to literature procedures. $CHCl_3$, CH_2Cl_2, 1,2 dichloroethane and $CDCl_3$ ware distilled over CaH_2, DMF was distilled under reduced pressure, 2-MTHF was distilled over Na.

NMR spectra were recorded on a Bruker Avance DRX 500 spectrometer. ^1H are reported relative to residual solvent signals and $^{31}P\{^1H\}$ chemical shifts are referenced to an external 85% H_3PO_4 (δ 0.00 ppm) sample. DOSY NMR experiments were carried out with solutions of 4 cm height to ensure gradient linearity along the samples. The temperature was controlled and kept at 298.0 ± 0.1 K. Data were acquired with 32 scans for each gradient step, 4 dummy scans and a linear gradient of 16 steps between 2% and 95%. Processing was carried out with Bruker's Topspin 2.1 software.

Absorption spectra were recorded on a Perkin-Elmer Lambda-16 spectrophotometer. Steady-state fluorescence spectra were performed by Perkin-Elmer model LS-50B and Edinburgh Instruments model FS-900 spectrophotometers. Fluorescence lifetimes (τ) were determined using the time correlated single-photon counter FL900, of the Edinburgh Instruments spectrophotometer. Fluorescence quantum yield measurements of the Bodipy-based compounds in 1,2 dichloroethane ($\eta(ClCH_2CH_2Cl) = 1.445$) were obtained relative to Rhodamine 6G in ethanol (Φ=0.94, η(EtOH) = 1.358).

Time-Resolved Fluorescence and Anisotropy Measurements: Femtosecond time-resolved fluorescence measurements were performed by means of the upconversion technique providing 150 fs temporal resolution. A Ti : Sapphire fs laser tuned at 760 nm was used as the light source where the second harmonic at 380 nm was employed for the excitation of the samples. For anisotropy measurements, the polarization plane of the excitation beam was changed by means of a Berek compensator. Nanosecond time-resolved fluorescence measurements were made using a Time Correlated Single Photon counting technique where a diode laser of 80 ps pulse duration at 400 nm was the excitation source. Detection was made by a multichanel plate photomultiplier and the instrument's response function was ~80 ps.

High Resolution Mass Spectrometry: Q-TOF high resolution mass spectrometer (Maxis Impact, Bruker Daltonics, Bremen, Germany) was applied for the HRMS spectra acquisition. The operating parameters of the electrospray ionization interface (ESI) in positive mode were: capillary voltage, 2800 V; end plate offset, 500 V; nebulizer, 0.5 bar; drying gas, 3 L min^{-1}; dry temperature, 180 C. The QTOF MS system recorded spectra over the range of m/z 500−8000 Da, with a scan rate of 1 Hz. The instrument provided a typical resolving power of 30,000−40,000. Mass spectra acquisition and data analysis was processed with DataAnalysis 4.1 (Bruker) and simulations were performed with SmartFormula Manually, a utility tool in vendor's software. The samples were dissolved in dichloromethane at a concentration of 100 μg/ml and they were directly infused in the system with a flow rate of 10 μl/min.

Calculations: Molecular modelling was performed in two steps: initially the structures were optimized using a molecular mechanics force field (UFF) and the output was minimized with the MOPAC2012 program[3] to full convergence (PM6 semiempirical method with the MOZYME function).

All simulations and fits to the experimental anisotropy decays were performed using the program "Scientist", version 3.0 of Micro Math.

Self-assembly of the tetragonal structure A2.

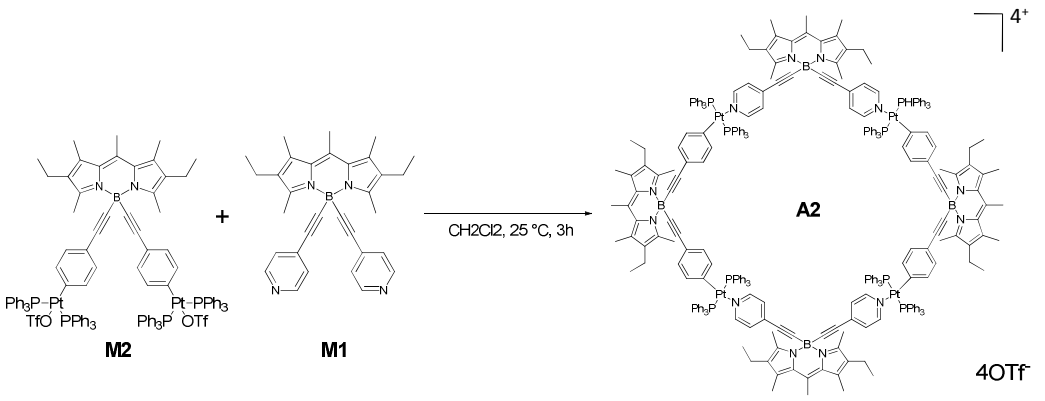

3.1 mg (0.006 mmol) of M1 were dissolved in 2.5 ml of CH_2Cl_2 in a 20 ml vial. A solution of 15.2 mg (0.006 mmol) of M2 in 5 ml of CH_2Cl_2 was added to the vial in 10 min with continuous stirring at rt. After 1 h the volume of the solution was reduced to 2 ml, and 1 ml of DMF was added. EtOAc was allowed to diffuse for 2 days and microcrystalline solid precipitated. The solid was washed twice with 5 ml of a 10:1 Et_2O/acetone mixture and dried. Yield 67% (12.3 mg).^{1}H NMR ($CDCl_3$): δ 7.97 (d, J=6.0 Hz, 8H), 7.30 (m, 120H), 6.62 (d, J=6.0 Hz, 8H), 6.54 (d, J=7.9 Hz, 8H), 6.35 (d, J=7.9 Hz, 8H), 2.71 (s), 2.64 (s), 2.59 (s), 2.57 (s), 2.46 (m) 2.37 (s), 2.33 (s), 1.07 (m, 24H); ^{31}P $\{^{1}H\}$ NMR ($CDCl_3$, 121.4 MHz): δ 20.82 (s, ^{195}Pt satellites, $^{1}J_{Pt-P}$=3047 Hz); ESI-MS: m/z 2552.860 $[M-2OTf]^{2+}$, m/z 1552.086 $[M-3OTf]^{3+}$.

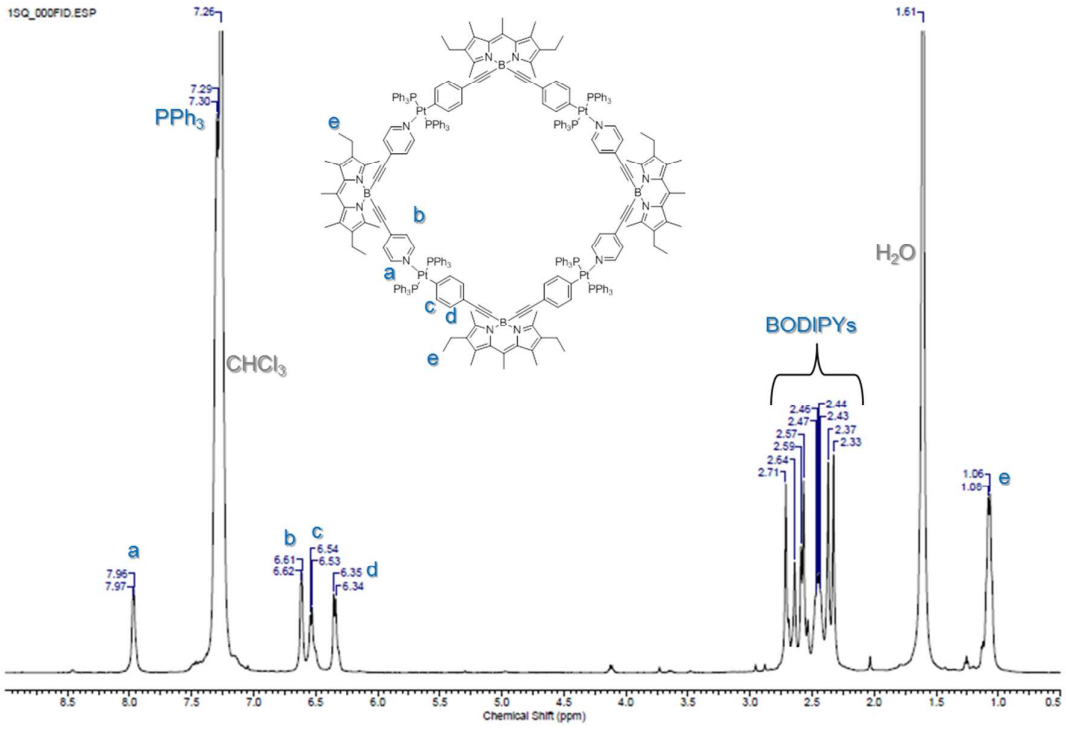

Figure S1. ^{1}H NMR (500 MHz) spectrum of A2 in $CDCl_3$.

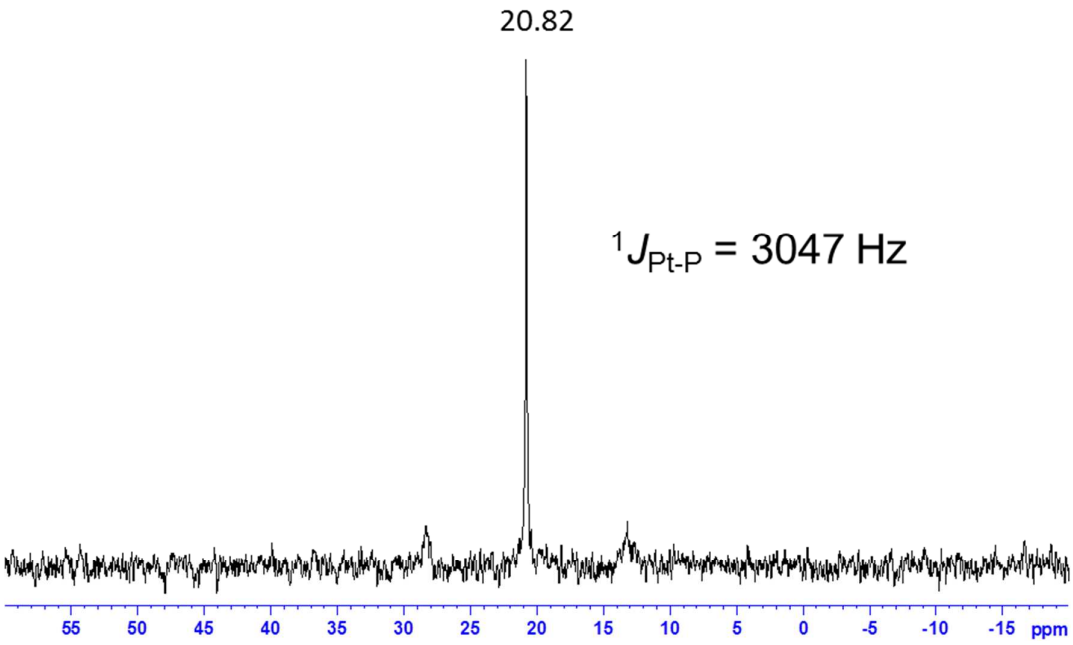

Figure S2. ^{31}P {^{1}H} NMR (121.4 MHz) spectrum of A2 in $CDCl_3$.

Self-assembly of the hexagonal structure A3.

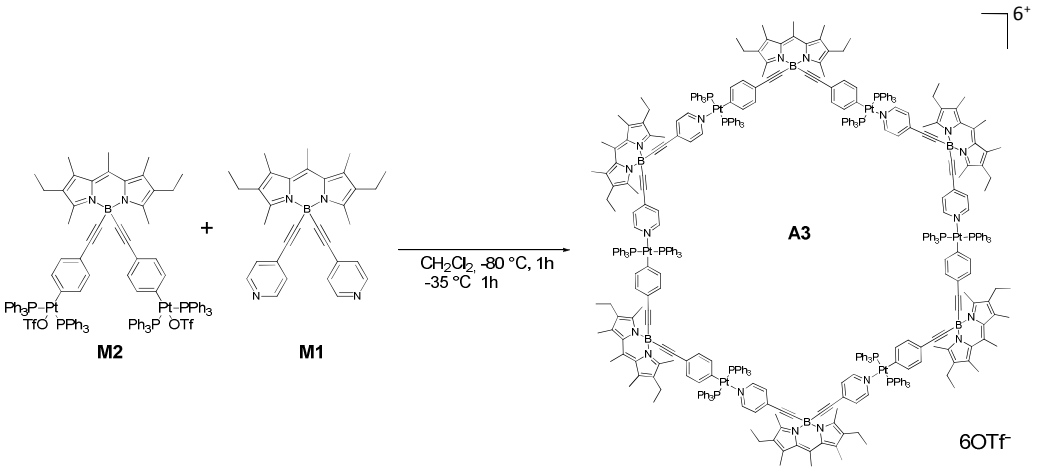

15.2 mg (0.006 mmol) of M2 were dissolved in 10 ml of CH_2Cl_2 in a 30 ml flask equipped with Ar inlet and cooled to -80 °C. Then 3.1 mg (0.006 mmol) of M1 were added with continuous stirring. The temperature was kept at -80 °C for 1 h, was elevated to -35 °C within 1 h and left to reach room temperature overnight under Ar. The volume of the solvent was reduced to 1 ml and 10 ml of Et_2O were added dropwise. The solid formed was separated by centrifugation, washed twice with 5 ml of a 10:1 Et_2O/acetone mixture and dried. Yield 84% (15.4 mg).^{1}H NMR ($CDCl_3$): δ 7.96 (s, 12H), 7.29 (m, 180H), 6.61 (s, 12H), 6.51 (s, 12H), 6.33 (s, 12H), 2.69 (s), 2.65 (s), 2.59 (s), 2.54 (s), 2.45 (s), 2.38 (s), 2.33 (s), 1.07 (m, 36H); ^{31}P {^{1}H} NMR ($CDCl_3$, 121.4 MHz) δ: 20.76 (s, ^{195}Pt satellites, $^{1}J_{Pt-P}$=3040 Hz); ESI-MS: m/z 1877.406 $[M-4OTf]^{4+}$,m/z 1472.171 $[M-5OTf]^{5+}$.

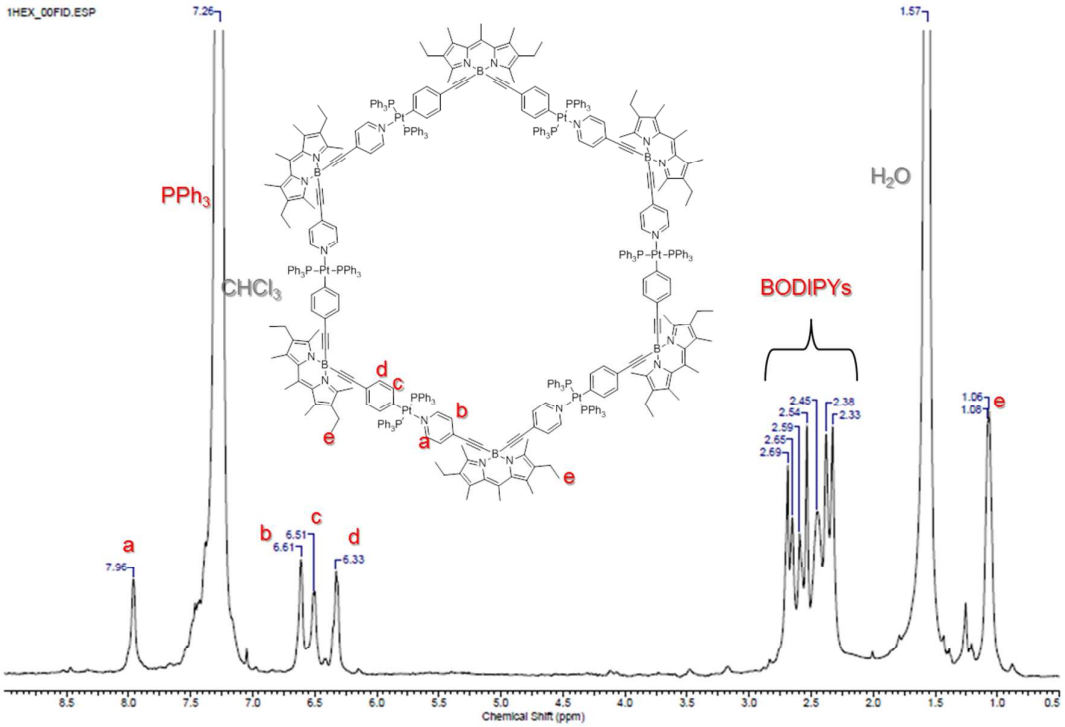

Figure S3. ^{1}H NMR (500 MHz) spectrum of A3 in $CDCl_3$.

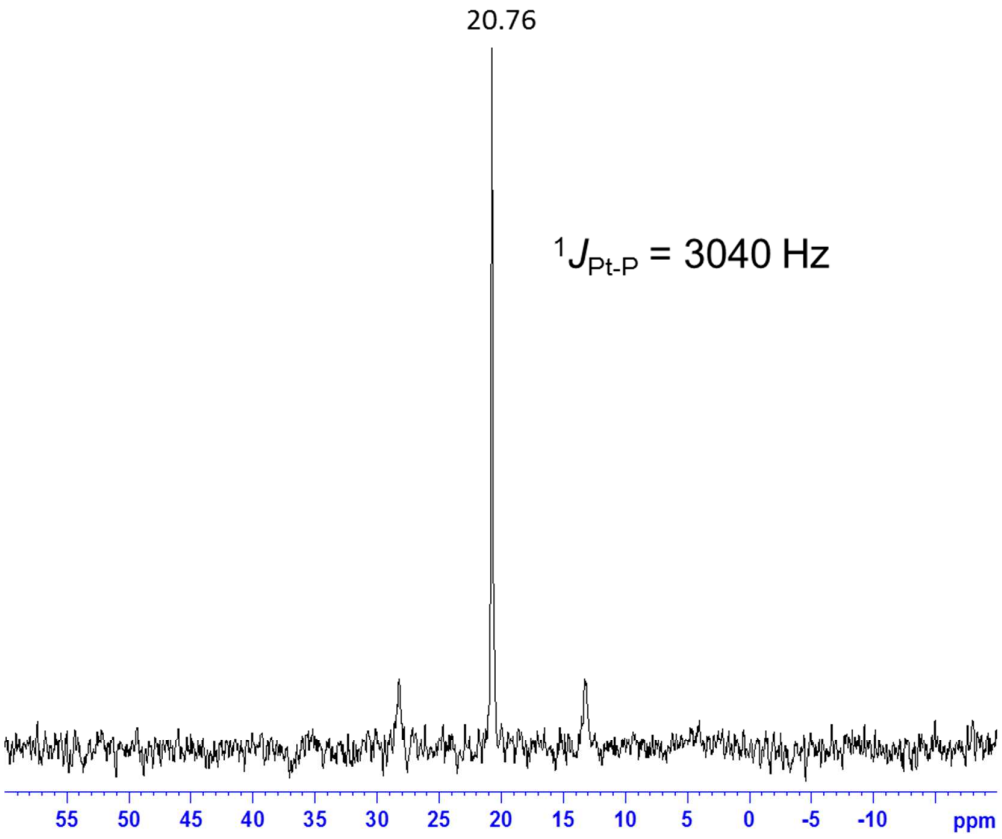

Figure S4. ^{31}P {^{1}H} NMR (121.4 MHz) spectrum of A3 in $CDCl_3$.

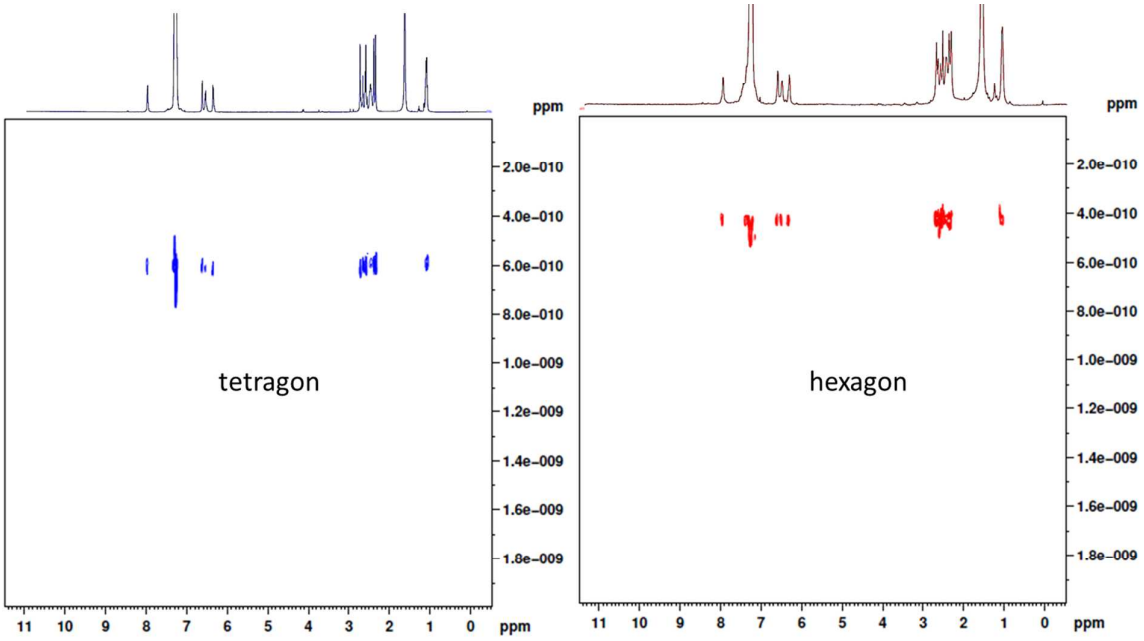

Figure S5. ^{1}H DOSY spectra (500 MHz, $CDCl_3$, 298 K) of A2 (tetragon) and A3 (hexagon).

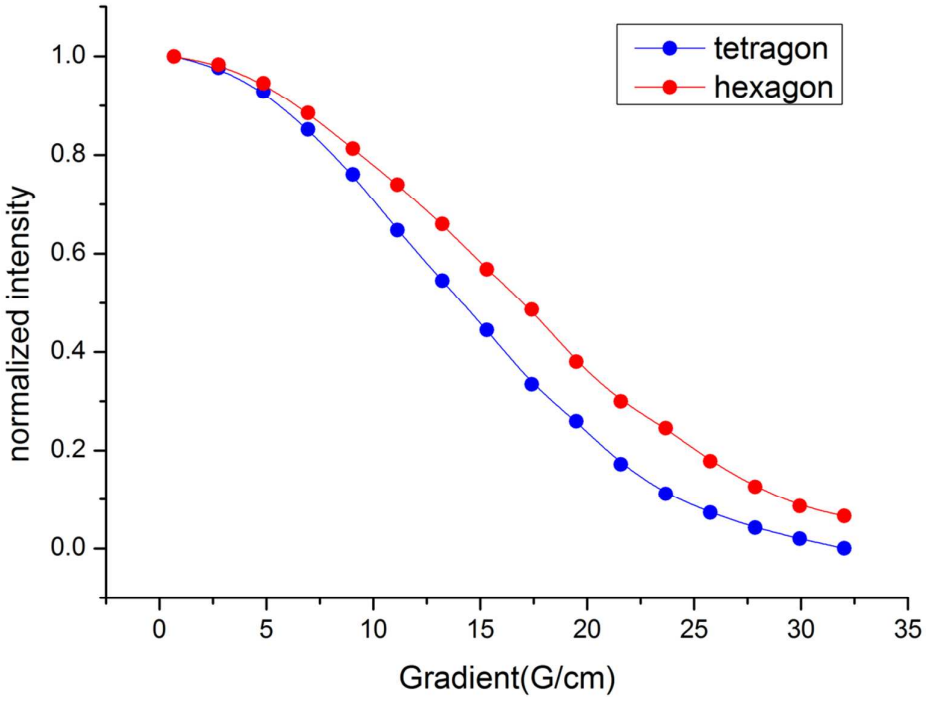

Figure S6. NMR diffusion decay curves of A2 and A3 in $CDCl_3$ from the experiments of figure S5. The intensity corresponds to integration of the area at 6.6 ppm.

The curves clearly demonstrate that A3 is larger than A2 (and diffuses slower) as they follow

the basic Pulsed field gradient NMR spectroscopy equation:

$$I = I_0 e^{-D\gamma^2 g^2 \delta^2 \left(\Delta - \frac{\delta}{3}\right)} \qquad (1)$$

where I is the observed intensity, I0 the reference intensity (normalized signal intensity), D the diffusion coefficient, γ the gyromagnetic ratio of the nucleus, g the gradient strength, δ the length of the gradient, and Δ the diffusion time.

The self – diffusion coefficient (*D*) for a spherical molecule is given by

$$D = \frac{kT}{6\pi\eta r_s} \qquad (2)$$

where k is the Boltzmann constant, T the temperature, η the viscosity of the solvent and r_s the hydrodynamic radius of the molecule. For a set of two molecules at the same temperature and solvent we have:

$$\frac{r_{s1}}{r_{s2}} = \frac{D_2}{D_1} \qquad (3)$$

Dipole – dipole Förster formulation

Within the framework of the dipole – dipole Förster formulation,[4,5] an effective interaction radius (R_0) can be calculated from the steady – state spectra and the fluorescence quantum yield of the donor chromophore (Φ_D) with the equations (4) and (5)

$$R_0^6 = 8.875x10^{-5} \frac{\kappa^2 \Phi_D}{n^4} J_{DA} \qquad (4)$$

where κ^2 is the *orientation factor* accounting for the orientation between the transition dipole moments μ_D, μ_A and their orientation with respect to the unit vector connecting the *D* and *A* centers (equation 9); *n* is the refractive index of the solvent (1.4448 for 1,2-dichloroethane) and J_{DA} is the spectral overlap integral defined by

$$J_{DA} = \frac{\int F_D(\lambda)\varepsilon_A(\lambda)\lambda^4 d\lambda}{\int F_D(\lambda) d\lambda} \qquad (5)$$

where $\varepsilon_A(\lambda)$ represents the molar extinction coefficient of the acceptor, and $F_D(\lambda)$ stands for the donor fluorescence spectrum normalized to unit area on a wavelength (λ) scale. By

considering either tecton **M1** or tecton **M2** as a donor, the corresponding calculated values of *R0* and J_{DA} are not changed noticeably (47.7 Å; 1.04772 x 10^{15} M^{-1} cm^{-1} nm^4 and 47.1 Å; 0.94948 x 10^{15} M^{-1} cm^{-1} nm^4 respectively) and are on a typical order of magnitude to be expected for Förster EET.

The *transition dipole moment* (μ) for the S0→S1 transition of the Bodipy dipoles was found to be equal in both tectons ($\mu_1 = \mu_2 = 6.6$ D) and was calculated from the absorption spectra using the relation of the dipole strength[6] (D)

$$D = \left|\vec{\mu}\right|^2 = 9.186x10^{-3} nf^{-2} \int \frac{\varepsilon(\bar{\nu})}{\bar{\nu}} d\bar{\nu} \qquad (6)$$

where n is the refractive index and $f = 3n^2/(2n^2+1)$ is the local-field correction factor.

In the limit of the dipole – dipole (Förster) mechanism, the EET rate constant k_{DA} is related through eq. 7 to the spectral overlap integral J_{DA} and the electronic coupling V_{DA} for coulombic interactions between the donor emission ($D^* \rightarrow D$) and acceptor absorption ($A \rightarrow A^*$) transition moments[7]

$$k_{DA} = \frac{2\pi}{\mathrm{h}} \left|V_{DA}\right|^2 J_{DA} \qquad (7)$$

The strength of Coulombic interactions V_{DA} between donor (D) and acceptor (A) transition dipoles, is given by the expression[7] (8),

$$V_{DA(calc)} = \frac{1}{4\pi\varepsilon_0} \kappa \frac{\left|\mu_D\right|\left|\mu_A\right|}{R_{DA}^{\ 3}} \qquad (8)$$

and is a function of the magnitudes of the transition dipoles $|\mu_D|$, $|\mu_A|$ and the orientational information involved in both the center-to-center separation R_{DA} and the orientation factor κ given by eq. (9)

$$\kappa^2 = (\cos\theta_{DA} - 3\cos\theta_D \cos\theta_A)^2 \qquad (9)$$

In the above expression, θ_{DA} is the angle between the donor's emission and acceptor's absorption transition moment, and θ_D and θ_A are the angles between these dipoles and the intermolecular separation vector R_{DA} joining the centroids of the donor and the acceptor.

Steady – State Excitation and Fluorescence Anisotropy Spectra

As Fig. S7 shows, the maximum possible anisotropy value, the so - called *limiting*[5] or *fundamental*[4] anisotropy r_0, was found to be $r_0 = 0.375 \pm 0.005$ across the entire range of the lowest electronic transition ($S_0 \rightarrow S_1$) of M**1.** The above value closely approximates the maximum theoretical value of 0.4 when the absorption and emission transition moment vectors are strictly collinear (i.e., due only to photoselection[4,5] 2/5=0.4; see equation 10). This indicates that the aforementioned vectors deviate by only $\theta \approx 10^0$ from being ideally collinear to each other.

$$r_0 = \frac{2}{5}\left(\frac{3\cos^2\theta - 1}{2}\right) \qquad (10)$$

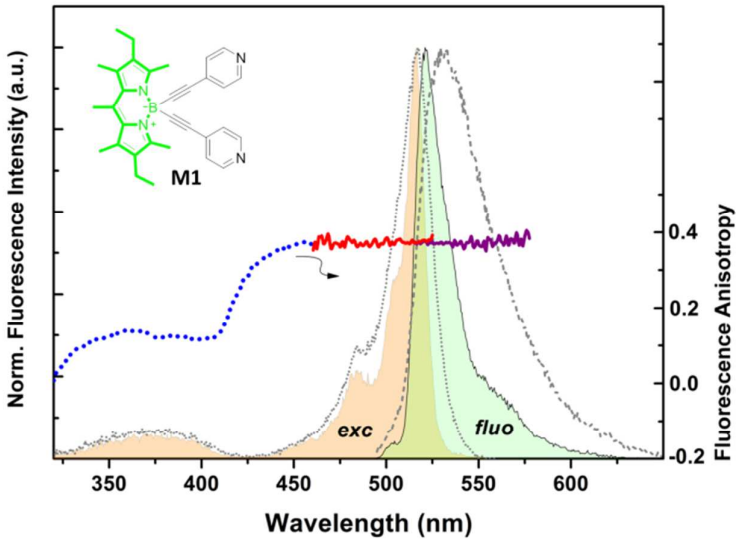

Figure S7. Low temperature (93 K; filled coloured) and room temperature (grey lines) excitation and fluorescence spectra of **M1** in 2-MTHF. Plot of the fluorescence anisotropy (*r*) *vs* the emission wavelength (mauve curve; exc: 500 nm). The excitation anisotropy spectrum has been recorded in two steps; to avoid large fluctuations of the spectrum in the 300 – 460 nm wavelength region (blue dotted line), wide slits (8.0 nm) were employed, instead of the typical slits (3.0 nm) used for the 460 – 525 nm (red solid line) wavelength window.

Dynamics of Intramolecular Excitation Energy Hopping

If depolarization due to rotational motion is negligible ($\Theta_{rot}^{-1} \approx 0$) at the time scale of the energy hopping, *the overall fluorescence anisotropy r(t)* is given by eq. 11

$$r(t) = r_d(t) + \sum r_i(t) \qquad (11)$$

where $r_d(t)$ is the anisotropy of the initially excited chromophore (donor) and $r_i(t)$ of the i_{th} acceptor given by eq. 12 and eq. 13, respectively.

$$r_d(t) = \frac{P_d(t)}{P_d(t) + \sum P_i(t)} r_{0d} \qquad (12)$$

$$r_i(t) = \frac{P_i(t)}{P_d(t) + \sum P_i(t)} r_{0a} = \frac{P_i(t)}{P_d(t) + \sum P_i(t)} d_T r_{0d} \qquad (13)$$

$P_d(t)$ and $P_i(t)$ stand for the excitation survival probabilities at time t following the exciting pulse, with the initial condition $P_d(0) = 1$ and $P_i(0) = 0$; d_T is the overall depolarization factor expressed as the product of all individual depolarizing factors of the acceptor's emission anisotropy with respect to the donor anisotropy r_{0d} ($r_{0a} = d_T x\, r_{0d}$) and is given by eq. 14

$$d_T = \left(\frac{3\cos^2\theta_{DA} - 1}{2}\right)\left(\frac{3\cos^2\theta_{AA} - 1}{2}\right) \qquad (14)$$

where θ_{DA} is the angle formed by the emission dipole moment of the donor and the absorption dipole moment of the emitting acceptor; θ_{AA} is the angle accounting for the slight deviation from collinearity between the absorption and emission transition moments of the emitting acceptor e.g., $\theta_{AA} \approx 10^0$ for M**1, M2**.

The time evolution of the excitation survival probabilities, after pulsed excitation of the B_1 (donor) at time t=0, can be described by the following coupled system of differential equations:

$$\frac{dP_d(t)}{dt} = -2k_{hopp}P_d(t) - \frac{1}{\tau_f}P_d(t) + k_{hopp}(P_2(t) + P_N(t)) \qquad (15)$$

and for i = 2, 3 …,N-1

$$\frac{dP_i(t)}{dt} = -2k_{hopp}P_i(t) - \frac{1}{\tau_f}P_i(t) + k_{hopp}(P_{i-1}(t) + P_{i+1}(t)) \qquad (16)$$

Long – Time (0 – 1 ns) Dynamics of r(t) for A1, A2 and A3

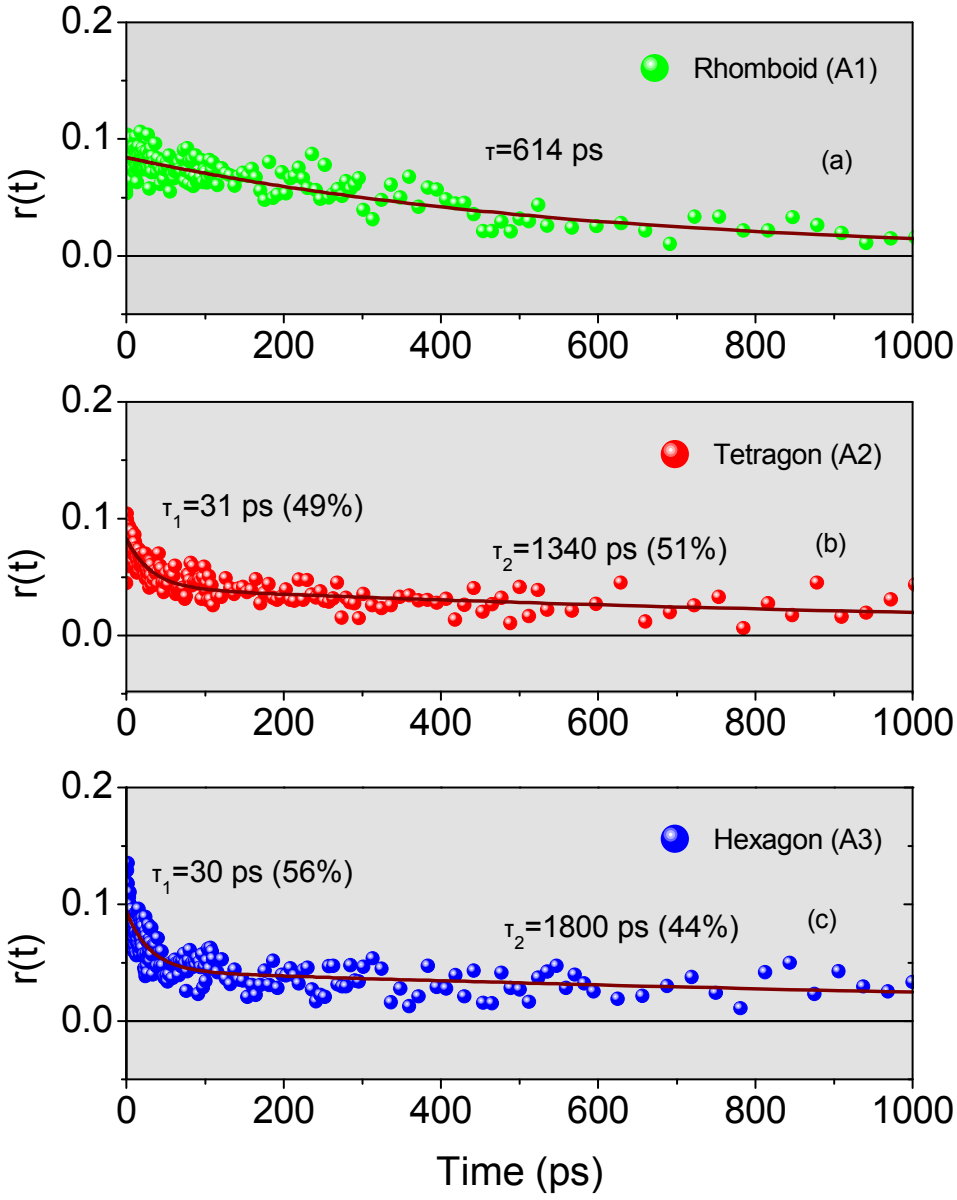

Figure S8. Long – time dynamics of *r(t)* for the estimation of the rotational correlation times of **A1**, **A2** and **A3**.

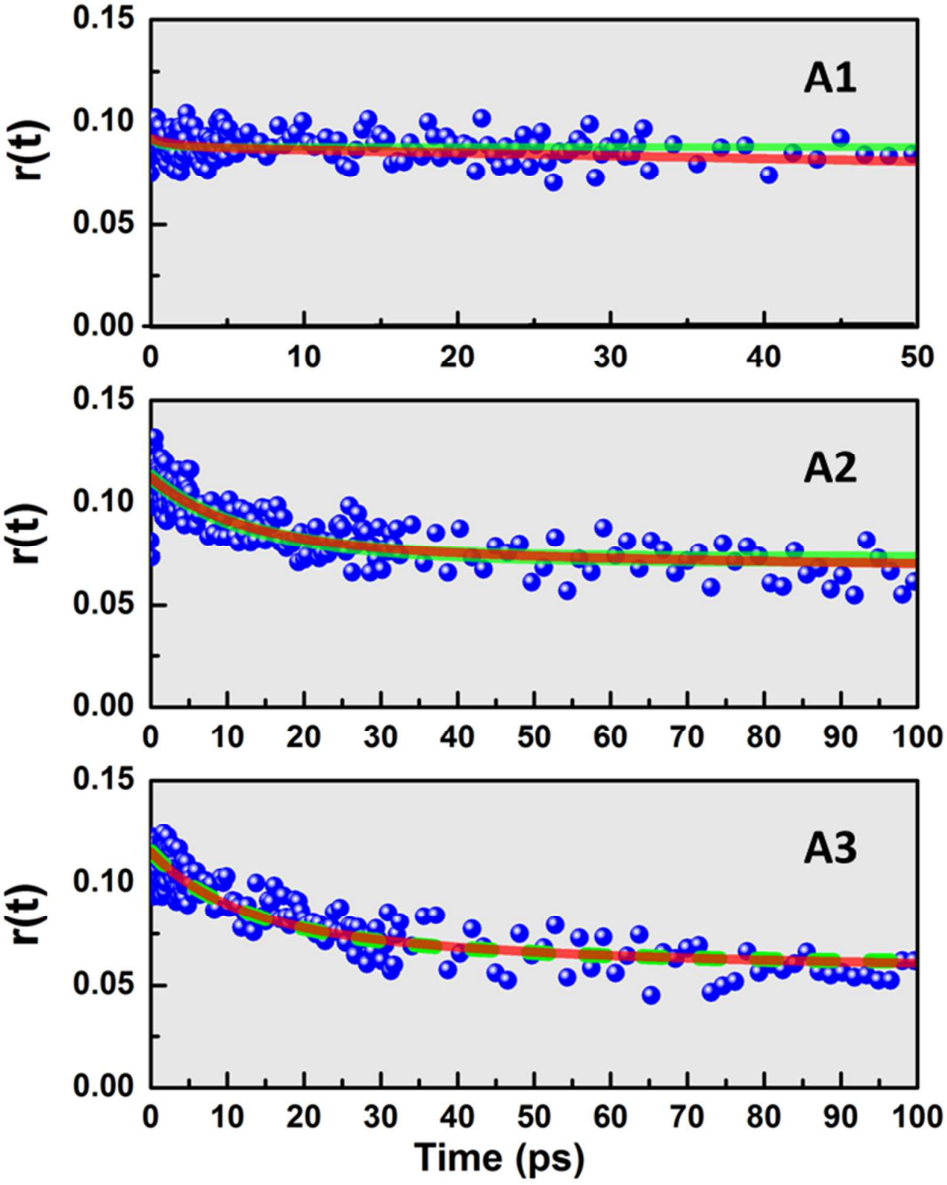

Figure S9. Simulated (upper panel) and fitting curves (middle and low panel) to the experimental anisotropy decay curves of **A1**, **A2** and **A3** by ignoring (green lines) and considering (red lines) the amount of depolarization due to the slow rotational motion.

References

1. Kaloudi-Chantzea, A.; Karakostas, N.; Raptopoulou, C. P.; Psycharis, V.; Saridakis, E.; Griebel, J.; Hermann, R.; Pistolis, G. Coordination-Driven Self Assembly of a Brilliantly Fluorescent Rhomboid Cavitand Composed of Bodipy-Dye Subunits. *J. am. Chem. Soc.* **2010**, *132*, 16327–16329.

2. Kaloudi-Chantzea, A.; Karakostas, N.; Pitterl, F.; Raptopoulou, C. P.; Glezos, N.; Pistolis, G. Efficient supramolecular synthesis of a robust circular light-harvesting Bodipy-dye based array. *Chem. Commun.* **2012**, *48*, 12213–12215.

3. MOPAC 2012, James J. P. Stewart, Stewart Computational Chemistry, Colorado Springs, CO, USA, HTTP://OpenMOPAC.net (2012).

4. Lakowicz, J. R. Principles of Fluorescence Spectroscopy, Kluwer Academic and Plenum Publishers, New York, **1999**.

5. Valeur, B. Molecular Fluorescence Principles and Applications, Wiley-VCH Verlag GmbH, **2001**.

6. Alden, R. G.; Johnson, E.; Nagarajan, V.; Parson, W. W.; Law, C. J.; Cogdell, R. G. Calculations of Spectroscopic Properties of the LH2 Bacteriochlorophyll−Protein Antenna Complex from Rhodopseudomonas acidophila. *J. Phys. Chem. B* **1997**, *101*, 4667−4680.

7. Krueger, B. P.; Scholes, G. D.; Fleming,G. R. Calculation of Couplings and Energy-Transfer Pathways between the Pigments of LH2 by the ab Initio Transition Density Cube Method. *J. Phys. Chem. B* **1998**, *102*, 5378−5386.